Saudi Journal of Biological Sciences 27 (2020) 3601–3614

Contents lists available at ScienceDirect

Saudi Journal of Biological Sciences

journal homepage: www.sciencedirect.com

Original article

Eco-friendly synthesis of silver nanoparticles from the whole plant of *Cleome viscosa* and evaluation of their characterization, antibacterial, antioxidant and antidiabetic properties

Suresh Yarrappagaari [a], Rajasekar Gutha [a], Lohitha Narayanaswamy [b], Lavanya Thopireddy [c], Lakshminarsimhulu Benne [a], Syed Siraj Mohiyuddin [c], V. Vijayakumar [b], Rajeswara Reddy Saddala [a,*]

[a] Division of Ethnopharmacology, Department of Biotechnology, School of Herbal Studies and Naturo Sciences, Dravidian University, Kuppam 517 426, Andhra Pradesh, India
[b] Centre for Organic and Medicinal Chemistry, VIT University, Vellore 632 014, Tamil Nadu, India
[c] Department of Zoology, Sri Venkateswara University, Tirupati 517 502, Andhra Pradesh, India

ARTICLE INFO

Article history:
Received 19 November 2019
Revised 28 July 2020
Accepted 30 July 2020
Available online 5 August 2020

Keywords:
Cleome viscosa
XRD
SEM
TEM
Antibacterial
Antioxidant
Antidiabetic

ABSTRACT

The current research is to develop an easy and eco-friendly method for the synthesis of three different concentrations of silver nanoparticles (1mMCvAgNPs, 2mMCvAgNPs and 3mMCvAgNPs) using aqueous whole plant extract of *Cleome viscosa* and to evaluate their antibacterial, antioxidant and antidiabetic properties. CvAgNPs were characterized by Using UV–vis spectrophotometer, X-ray diffraction (XRD), Fourier transform infrared spectroscopy (FT-IR), scanning electron microscope (SEM) and transmission electron microscope (TEM). The formation of CvAgNPs was confirmed by the observation of band between 250 nm to 600 nm UV–vis spectrum. The crystalline structure of CvAgNPs with a face-centered cubic (FCC) was confirmed by XRD. The responsible phytochemicals for the reduction and capping material of CvAgNPs were observed with FT-IR. The SEM analysis confirmed the size and shapes of CvAgNPs. The CvAgNPs have shown the rich content of total phenolic and total flavonoid components. The CvAgNPs have shown significant antibacterial activity on multi drug resistance Gram-negative and Gram-positive bacteria and also have shown significant strong antioxidant activities (DPPH, ABTS, H_2O_2 scavenging, Phosphomolybdenum assay and reducing power). The inhibitory action of CvAgNPs on α-glucosidase and α-amylase was stronger than the inhibitory action of acarbose. To best of our knowledge, this is the first attempt on the synthesis of AgNPs using *C. viscosa* whole plant aqueous extract. The synthesized CvAgNPs exhibited good antimicrobial, antioxidant and antidiabetic properties. Hence, to validate our results, the *in vivo* studies at the molecular level are needed to develop *Cleome viscosa* as an antibacterial, antioxidant and anti-diabetic agent.

1. Introduction

Currently, researchers are fascinated by the rising of a well-organized process for the synthesis of nanoparticles (NPs) in large-scale. 1–100 nm molecule sizes are considered as nanoparticles (Khan et al., 2017). Nanomedicine is a rapidly developing branch of therapeutics in the biomedical field and is capable of formulating finest nanoparticles from metals such as silver (Ag), gold (Au) and platinum (Pt). Among these metal-NPs, silver nanoparticles (AgNPs) are considered as most suitable for to the surface plasmon resonance (SPR), which can be effectively seen by UV–vis spectrophotometer (Chaudhari et al., 2019). Ag is a general cost-effective, regularly utilized metal in our daily lives and also an antimicrobial agent. Because of the above-mentioned reasons, Ag has been used in the synthesis of NPs which has a broad range of usages such as preparation of food dispensation, contemporary ointment and therapeutic insert (Karthik et al., 2013).

Synthesis of AgNPs through physical and chemical techniques results in the Utilization of enormous and dangerous synthetic substances and also required high temperature (Quaresma et al., 2009). The nanoparticles synthesis by the biological process using plants or plant extracts, micro-organisms and enzymes are highly

* Corresponding author at: Division of Ethnopharmacology, Department of Biotechnology, Dravidian University, Kuppam 517 426, India.
E-mail address: drsrr2017@gmail.com (R.R. Saddala).
Peer review under responsibility of King Saud University.

Production and hosting by Elsevier

https://doi.org/10.1016/j.sjbs.2020.07.034
1319-562X/

recommended so green-synthesis is a good alternative for physical and chemical methods (Kuppusamy et al., 2016; Iravani et al., 2014). Biological agents such as plants, parasites, bacteria's and viruses can assimilate and absorb metals and also can be utilized as decreasing operator and controls the particles of metal nanostructural position. The method of green synthesis of AgNPs using biological agents is straightforward, solid, nontoxic and eco-accommodating (Singh et al., 2018; Selvam et al., 2017). Green synthesis of AgNPs by different therapeutic plants include, *Berberis vulgaris* (Behravan et al., 2019), *Calophyllum tomentosum* (Govindappa et al., 2018), *Sonneratia apetala* (Nagababu and Rao, 2017), *Calliandra haematocephala* (Raja et al., 2017), and *Helicteres isora* (Bhakya et al., 2016), have been reported to demonstrate *in vitro* antioxidant, antibacterial and antidiabetic activities. Based on the above-mentioned research, the present study was designed to the synthesis of AgNPs with *Cleome viscosa* whole plant aqueous extract and to evaluate their antibacterial, antioxidant and antidiabetic properties.

Previous investigations reported that the utilization of various plant parts, for example, leaf, root, stem, bark, bud, fruit and latex for silver nanoparticles synthesis. Up to now a lot of work has been done in green synthesis method for plant-mediated formulation of silver nanoparticles and the exploration for the roles of phytochemicals for various plants. Flavonoids, phenols, alkaloids, terpenoids, amides, aldehydes, terpenoids, carboxylic acid, and ketones were the most important phytochemicals engaged in the reduction of silver were distinguished by spectroscopic examinations (Rai et al., 2014; Hembram et al., 2018). A few phytochemicals, for example, flavones, quinones were found and recognized as water dissolvable which are responsible for the rapid reduction process. In addition, the reduction properties of plants secondary metabolites are attributed to the higher potential ability of plant extracts to synthesize nanoparticles with improved characteristics (Ahmed and Mustafa, 2020). In the synthesis of silver nanoparticles, plant extracts act as a reducing agent for reducing Ag^{+} to Ag^{0} and capping or stabilizing agents for preventing the aggregation of the nanoparticles.

Cleome viscosa (Cleomaceae) is a traditional edible medicinal plant commonly known as Asian spider flower and grows in major part of the world. Leaves and young shoots are cooked as a vegetable (Manandhar, 2002). The seedpods are utilized to prepare pickles (Facciola, 1990). In the system of Ayurveda, the extracts are proficient to treat malaria, snake bites, hypertension and diarrhea sickness. Visconoside-C, quercetin, astragalin, kaempferol and kaempferitrin were isolated from the leaves of *C. viscosa* which exhibited hepatoprotective action against CCl_4-initiated hepatotoxicity (Nguyen et al., 2017). Quercetin 3-O-(2″-acetyl)-glucoside identified in *C. viscosa* exhibited strong antimicrobial and inflammation property (Senthamilselvi et al., 2012).

Recently, Lakshmanan et al. (2018) and Pannerselvam et al. (2020) used *C. viscosa* fruit and leaves extract for the synthesis of AgNPs and also evaluated their antibacterial activity and potential cytotoxic effects against human breast carcinoma cells. However, the investigation of AgNPs synthesized by traditional edible medicinal plants, particularly in *C. viscosa* is very much limited. Thus, the current study was aimed to AgNPs synthesis from edible *C. viscosa* plant aqueous extract as a reducing and stabilizing agent and to determine the qualitative and quantitative phytochemical analysis of synthesized AgNPs. Considering the significance of AgNPs and its biomedical applications, we focused on the biosynthesis of stable AgNPs from *C. viscosa* whole plant aqueous extract by utilizing bioreduction technique. The produced AgNPs would be characterized using UV–vis, XRD, FT-IR and SEM with EDX (Energy dispersive x-ray) and TEM techniques. Furthermore, synthesized AgNPs were described and assessed for antibacterial, antioxidant and antidiabetic activity.

2. Material and methods

2.1. Chemicals and reagents used

Folin-Ciocalteu's reagent, sodium carbonate, aluminium chloride, potassium acetate, quercetin, Mueller-Hilton agar medium, DPPH (2,2-diphenyl-1-picrylhydrazyl), ABTS (2,2′-azino-bis(3-ethylbenzothiazoline-6-sulfonic acid)), potassium persulfate, ammonium molybdate, trisodium phosphate, potassium ferrocyanide, glucose, hemoglobin, sodium azide, 3, 5-dinitrosalicylic acid, ascorbic acid and α-amylase were purchased from Himedia (Bangalore, India). α- glucosidase, *p*-NPG (p-nitro phenyl α-d-glucopyranoside)), gallic acid, acarbose was purchased from Sigma–Aldrich (Bangalore, India). Standard anti-microbial drug, gentamycin and antidiabetic drug, metformin were purchased from the local market. All other chemical reagents and buffers were used as an analytical grade in this study.

2.2. Collection of plant, validation and extract preparation

We Collected the whole plant of *C. viscosa* from Dravidian University region of Kuppam of Andhra Pradesh, India, during the rainy season and the plant was validated with the help of taxonomist, Prof. N. Yasodamma, Tirupati, Andhra Pradesh, India. Water was used as a solvent for the extraction of whole plant powder of *C. viscosa* in microwave method with two cycles for 10 min at 100 °C. To find the responsible secondary phytochemicals present in the aqueous extract, qualitative phytochemical screening was performed (Al-Owaisi et al. (2014); Sheel et al. (2014); Trease and and Evans (2002)).

2.3. Synthesis and characterization (UV–vis, XRD, FT-IR and SEM with EDX and TEM) of CvAgNPs

5 g of dried whole plant of *C. viscosa* powder was added with 20 mL of distilled water. The *C. viscosa* solution was concentrated at 100 °C for 10 min. The aqueous extract was mixed with 10 mL of different concentrations of 1 mM $AgNO_3$, 2 mM $AgNO_3$ and 3 mM $AgNO_3$ solution at 26 ± 2 °C temperature. After 1 h, we observed the colour change of the post-mixtures from light green into dark brown.

Formation of CvAgNPs was confirmed by UV–visible spectral analysis. The absorbance spectra was recorded using UV–vis spectroscopy (JASCO-V-670, Japan.) at the wavelength between 200 and 600 nm. The FT-IR (Fourier-transform infrared spectroscopy) spectroscopy analysis was performed (Thermo Nicolet-330, Madison, WI, USA) to distinguish the potential functional groups at biomolecules present in the synthesized CvAgNPs. The XRD (X-Ray Diffraction) spectrum of CvAgNPs was confirmed by using X-ray diffracts range, it was (Panalytical Xpert-PRO 3050/60) worked at 30 kV with 100 mA and range was confirmed by using Cu-Kα waves. The size of the particle and exterior morphology of biosynthesized CvAgNPs were deliberated by SEM (Scanning electron microscope) (ZEISS-EVO18, USA) and EDX (Energy-dispersive X-ray) (NOVA-450 instrument). JEOL JEM 2100 High-Resolution Transmission Electron Microscope (TEM) was utilized for the imaging and SAED (Selected Area Electron Diffraction) pattern through a step up the 200 kV voltages.

2.4. Determination of phytochemical contents in synthesized CvAgNPs

2.4.1. Total phenol content (TPC)

Total phenolic content (TPC) was calculated according to the standard Singleton and Rossi (1965) procedure. 100 mg/mL of synthesized CvAgNPs and gallic acid standard were mixed with

Folin–Ciocalteu's reagent (0.5 mL) and 20% of sodium carbonate (2.5 mL) in addition to 6.0 mL of distilled water. The resulting solution was mixed well and incubated at 40 °C for 30 min by using water bath shaker. The reaction mixture absorbance was measured at 760 nm. A calibration curve was prepared by using gallic acid standard.

2.4.2. Total flavonoid content (TFC)

For the determination of total flavonoid content (TFC), aluminium chloride colourimetric method was employed by using Chang et al., (2002). The 50–100 mg/mL concentration of quercetin standard was used for the construction of the calibration curve. In brief, 100 mg of three different concentrations of synthesized CvAgNPs were dissolved in 1 mL of distilled water individually. 0.5 mL of this solution was mixed with 95% ethanol (1.5 mL), 10% aluminum chloride (0.1 mL), 1 M potassium acetate (0.1 mL) in addition to distilled water (2.8 mL). After incubation at room temperature (26 ± 2 °C) for 30 min, the reaction mixture absorbance was measured at 415 nm.

2.5. Antibacterial activity of the synthesized CvAgNPs

2.5.1. Bacterial strains used in this study

The antibacterial strength of each CvAgNPs (1 mM, 2 mM and 3 mM) was assayed by using five bacterial strains. Four strains of Gram-negative (*Klebsiella pneumoniae*, *Pseudomonas aeruginosa*, *Escherichia coli*, *Pseudomonas putida*) and one strain of Gram-positive (*Staphylococcus aureus*) bacteria were used. The strains were collected from the Microbiology Department, P.E.S Medical College, Kuppam, India.

2.5.2. Inoculums preparation

Bacterial strains were sub cultivated at 35 °C for overnight into Mueller-Hilton agar slants. The growth of bacteria was collected using 5 mL of sterile water.

2.5.3. Antibacterial activity of synthesized CvAgNPs

The disk diffusion technique is utilized to evaluate the antibacterial activity of the synthesized CvAgNPs. 10 mL of agar medium (Mueller-Hilton) was poured into disinfected Petri-dishes followed by 15 mL of the earlier prepared bacterial suspension. Filter paper discs loaded with 10 mg/mL of CvAgNPs were placed on the top of the agar plates. Positive control Gentamycin (5 μg) was loaded on the filter paper disc. The petri-plates were held in the refrigerator at 4 °C for 120 min to allow CvAgNPs diffusion/dispersion then incubated at 35 °C for 24 hrs. The inhibition zones were indicated as antibacterial activity.

2.6. Antioxidant activity of synthesized CvAgNPs

2.6.1. Assay of DPPH radical scavenging activity

The antioxidant activity of the CvAgNPs was measured based on the DPPH free radical scavenging activity according to Brand-Williams et al., (1995) method with slight modifications. 1 mL of 0.1 mM DPPH in methanol was mixed with 1 mL of CvAgNPs solution of various concentrations (20, 40, 60, 80 and 100 μg/mL). Consequently, 1 mL of methanol and 1 mL of DPPH was used as control and gallic acid was used as the reference standard. The reaction was conceded in three times and the absorbance was measured at 517 nm after incubation of 30 min in dark.

2.6.2. Assay of ABTS radical scavenging activity

The assay of ABTS radical scavenging activity was adopted from Re et al., (1999). The stock solution included 7 mM of ABTS and 2.4 mM of potassium persulfate. 1 mL of varying concentrations (20, 40, 60, 80 and 100 μg/mL) of the CvAgNPs and standard ascorbic acid were permitted to react with 1 mL of ABTS and the absorbance was measured at 734 nm after the incubation for 7 min.

2.6.3. Assay of H_2O_2 radical scavenging activity

The ability of the CvAgNPs to scavenge H_2O_2 was determined according to the Ruch et al., (1989) method. 2 mmol/l of H_2O_2 solution was prepared in neutral phosphate buffer. Synthesized CvAgNPs (20, 40, 60, 80 and 100 μg/mL) were added to 0.6 mL of H_2O_2 solution. The absorbance of H_2O_2 was measured at 230 nm after incubation of 10 min against blank and the radical scavenging activity was compared with ascorbic acid.

2.6.4. Assay of phosphomolybdenum method

The total antioxidant activity of the CvAgNPs was estimated by the phosphomolybdenum method explained by Prieto et al., (1999). 1 mL of each CvAgNPs (20, 40, 60, 80 and 100 μg/mL) was added with 3 mL of reagent (0.6 M H_2SO_4, 28 mM Na_3PO_4 and 4 mM of Ammonium molybdate reagent). Consequently, 4 mL of reagent solution was used as control/blank and ascorbic acid was used as a reference standard. The reaction mixture was incubated at 95 °C for 150 min. After the mixture was cooled at room temperature and absorbance was measured at 695 nm.

2.6.5. Total reducing power ability

The ability of reducing power of CvAgNPs was determined according to the Oyaizu, (1986) method. Different concentrations (20, 40, 60, 80 and 100 μg/mL) of the CvAgNPs in 1.0 mL of sterile distilled water was added with 2.5 mL phosphate buffer (0.2 M; pH 6.6), 2.5 mL potassium ferrocyanide (1%) and mixture was incubated at 50 °C for 20 min. In addition, 2.5 mL TCA (10%) was mixed with the reaction mixture and centrifuged at 3000 rpm for 10 min. 2.5 mL of the upper layer solution was mixed with 0.5 mL $FeCl_3$ (0.1%) and the absorbance was measured at 700 nm.

2.7. In vitro antidiabetic activity of synthesized CvAgNPs

2.7.1. The activity of α-glucosidase inhibition

1 mg of the α-glucosidase enzyme (isolated from *Saccharomyces cerevisiae*) was suspended with 100 mL neutral PBS buffer which contains the 200 mg of bovine serum albumin (Yin et al., 2008). The various concentrations (20, 40, 60, 80 and 100 μg/mL) of CvAgNPs were added with reaction mixture (10 μL of pH 6.8 phosphate buffer; 490 μL of 5 mM *p*-NPG (p-nitro phenyl α-d-glucopyranoside). The reaction mixture was incubated at 37 °C for 5 min then add 250 μL of α-glucosidase (0.15 unit/mL) and again incubated at 37 °C for 15 min. Then cool the reaction and add 2 mL of sodium carbonate (200 mM) to stop the reaction. The activity of enzyme inhibition was measured at 405 nm and acarbose was utilized as a reference compound.

2.7.2. The activity of α-amylase inhibition

In 1% phosphate buffer and starch solution was prepared and incubated with 500 μL enzyme (α-amylase) for 10 min at 37 °C. 1 mL (20, 40, 60, 80 and 100 μg/mL) of synthesized CvAgNPs was added to the enzyme solution. 2 M of NaOH is applied to stop the reaction process. 1 mL of Dinitro salicylic acid is assorted and the reaction is maintained in the hot water bath for 5 min. After completion of incubation, test tubes were cooled by running tap water, the final volume of test solution was makeup to 10 mL using sterile distilled water and absorbance was measured at 540 nm. Acarbose was used as a reference substance (Hansawasdi et al., 2000).

2.7.3. Assay of non-enzymatic glycosylation of hemoglobin (HbA1c)

In vitro antidiabetic activity of synthesized CvAgNPs was scrutinized with the HbA1c method (Chaudhari et al., 2013). The

combination of 2% glucose, 0.06% haemoglobin and 0.02% sodium azide solutions were organized in 0.01 M phosphate buffer (pH 7.4). 1 mL of different concentrations (20, 40, 60, 80 and 100 μg/mL) of CvAgNPs was mixed with above combination. The reaction mixture was incubated in a dark place at room temperature for 72 hrs. The levels of HbA1c were measured at 520 nm. Metformin was used as a reference drug for this assay.

2.8. Method of calculation for scavenging and inhibitory activity

The obtained absorbances of *in vitro* antioxidant assays (DPPH, ABTS, H_2O_2, Phosphomolybdenum method, and reducing power ability) and *in vitro* antidiabetic assays (α-glucosidase inhibition, α-amylase inhibition and HbA1c levels) were estimated by the following formula;

$$\text{Percentage of free radical scavenging/inhibitory activity} = (\text{Ac}) - (\text{As})/(\text{Ac}) \times 100$$

whereas Ac- Absorbance of control; As- Absorbance of the test sample (CvAgNPs).

2.9. Statistical analysis

The total data included in this work were subjected to a one-way ANOVA for Mean ± SE (n = 3) and the significant difference between the means of treated groups were determined by Tukey's post hoc test ($P < 0.05$) using SPSS software (SPSS version 16.0, SPSS Inc. Chicago, IL, USA).

3. Results and discussion

3.1. Screening of qualitative phytochemicals

Phytochemical screening of aqueous extract of the whole plant of *C. viscosa* was presented in Table 1. Phytochemical screening demonstrated the nearness of alkaloids, sugars, coumarins, flavonoids, glycosides, proteins and amino acids, saponins, steroids, phenols and tannins. The nearness of these organically active compounds may assume a major role in capping and stabilization of AgNPs (Oluwaniyi et al., 2016).

3.2. Synthesis of CvAgNPs

Current worldwide interest for the utilization of eco-friendly and cost-effectiveness push the utilization of incredible medicinal plants to organize the green synthesis of AgNPs, that have various organic and reactant properties. The present study dealt with the synthesis, characterization, quantifications of phytochemical contents, antibacterial, antioxidant and antidiabetic activities of CvAgNPs.

The green synthesized AgNPs are commonly demonstrated with their range, shape, and surface area with dispersity. When the whole plant of aqueous extract was mixed with three different concentrations i.e. 1mM$AgNO_3$, 2mM$AgNO_3$ and 3mM$AgNO_3$ and incubated at 26 ± 2 °C, from 30 min to 1 h of time, changed its color from brown to dark-brown (Fig. 1), signifying the formation of 1mMCvAgNO_3, 2mMCvAgNO_3 and 3mMCvAgNO_3. It was a proficient and fast technique, which was very much clarified by different scientists who worked with various plant frameworks (Bharathi et al., 2018; Bhakya et al., 2016). Color change was observed due to the action of surface plasmon resonance in AgNPs (Anandalakshmi et al., 2016). Our outcomes are similar to Govindappa et al. (2018), who reported the development of AgNPs within 30 min of incubation. However, Balavijayalakshmi and Ramalakshmi, (2017) stated that colour change was observed after 24 h of performance the moderate decrease of the $AgNO_3$ by the solvent extract of *Carica papaya*.

3.3. Characterization of CvAgNPs using UV–vis, XRD, FT-IR, SEM with EDX and TEM analysis

The aqueous extract colour was changed from brown to dark-brown after adding of 1 mM $AgNO_3$, 2 mM $AgNO_3$ and 3 mM $AgNO_3$ from 30 min to 1 h, afterwards no more colour alterations were observed up to 24 h of incubation in three concentrations (Fig. 1). This might be due to the presence of high content of phenols and flavonoids in the whole plant aqueous extract of *C. viscosa* which reduced silver to AgNPs owing in the direction of surface plasmon resonance of synthesized CvAgNPs. Bioreduction of Ag+ ions were pragmatic in the 1 mM $AgNO_3$, 2 mM $AgNO_3$ and 3 mM $AgNO_3$ solutions from *C. viscosa* chemical compounds. Fig. 2 shows the UV–vis absorption spectra of synthesized 1mMCvAgNPs, 2mMCvAgNPs and 3mMCvAgNPs. It was observed that the maximum absorbance of all synthesized CvAgNPs occurs at 434 nm range, it represents that the AgNPs were formed. Similar results were observed for *Aloe Vera* leaf extract (Ashraf et al., 2016), it specified the development of AgNPs.

The CvAgNPs crystalline nature was confirmed by XRD analysis (Fig. 3). The XRD showed the evidence of diffraction peaks at [111], [200], [220] and [311] appearing at 2θ. These peaks indicate the crystalline face-centered cubic (FCC) nature of the three CvAgNPs which is in concurrence with the catalog of the Joint Committee on Powder Diffraction Standards. The intense of extra peaks at 2θ points of CvAgNPs are a result of the association of $AgNO_3$ which was utilized for the synthesis of AgNPs (Rajakumar et al., 2017; Taha et al., 2019). The expanding of Bragg's peaks shows the arrangement of nanoparticles and Debye-Scherrer's condition ascertains the mean size of the AgNPs was 24 nm. The examples of XRD propose that crystallization of the bioorganic stage happens on the outside of AgNPs. Our outcomes are in confirmation with the results of Rajakumar et al. (2017) and Taha et al. (2019).

The SEM images of the biosynthesized three different concentrations of CvAgNPs at different enlargements are exposed in Fig. 4. It was found that CvAgNPs were rod-shaped, spherical, and triangular in shape (Fig. 4A–C). Fig. 4A confirmed the biomolecular outside layer on the layer of AgNPs surface, which is liable in favor to improve the AgNPs stability. The SEM micrograph is shown in Fig. 6A, B and C established and confirmed the attendance of metal AgNPs. Our outcomes are confirmed with the results of Jyoti et al. (2016).

Table 1
Screening of phytochemicals of aqueous extract of *C. viscosa* whole plant.

Phytochemicals	Aqueous extract
Alkaloids	+
Anthraquinones	–
Carbohydrates	+
Coumarins	+
Flavonoids	+
Gums	–
Glycosides	+
Oils and fates	–
Proteins and amino acids	+
Saponins	+
Steroids	+
Phenols	+
Reducing sugars	–
Tannins	+

+ Sign means presence and –Sign signifies nonappearance

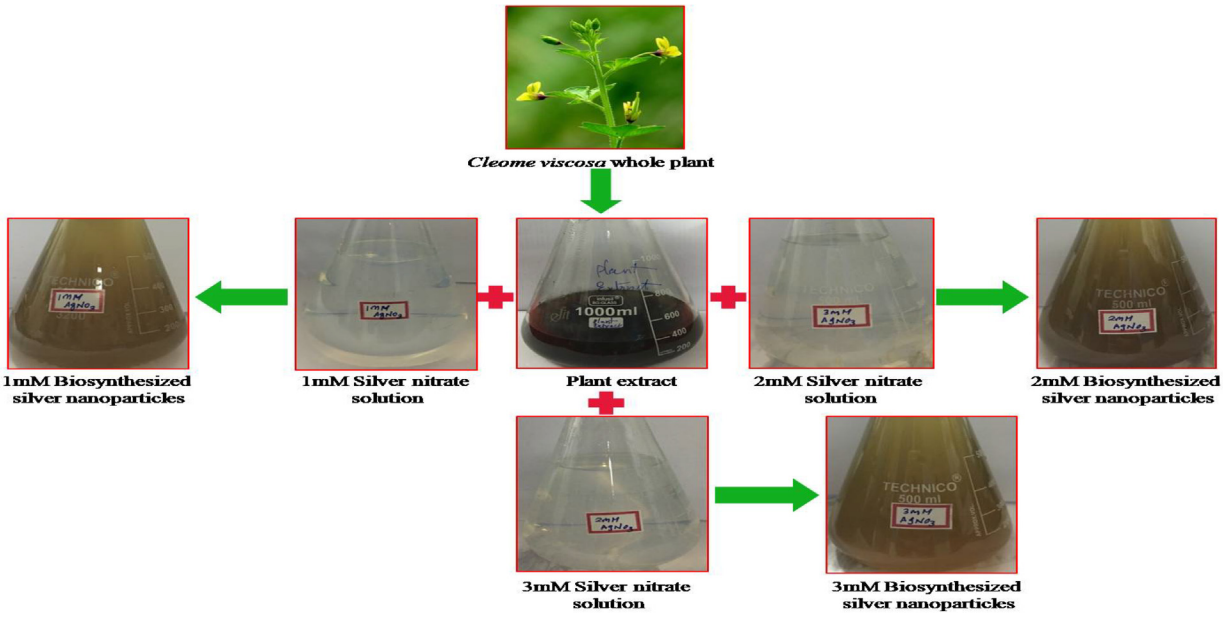

Fig. 1. Schematic diagram of biosynthesis of CvAgNPs.

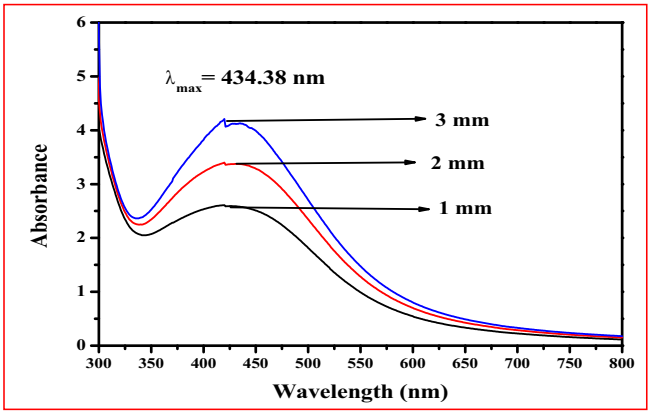

Fig. 2. UV–vis absorption spectrum of synthesized 1mMCvAgNPs, 2mMCvAgNPs and 3mMCvAgNPs.

Fig. 5 represents the EDX spectrum of the CvAgNPs recommend the attendance of silver (Ag) as the major feature element. Metallic AgNPs commonly show a characteristically strong indication peak at 3 keV, due to the surface plasmon resonance (Anandalakshmi et al., 2016). Fig. 5 gives on qualitative information of biosynthesized CvAgNPs. Observed the attendance of elements i.e. C (4.59%), O (11.13%) and Ag (84.28%) at different atomic percentage (20.55%, 37.43% and 42.03%). The biosynthesized AgNPs demonstrate strong significance in the ranges of 3–4 keV (Ismail et al., 2018).

The TEM micrographs of the biosynthesized CvAgNPs magnifications are shown in Fig. 6A–C. It was found that CvAgNPs were rod-shaped, spherical, and triangular in shape with maximum particles in the size range of 50 nm (Fig. 6C). Fig. 6B and C confirmed the biomolecular covering on the exterior layer of CvAgNPs, which are liable to improve the steadiness of AgNPs. The SAED model confirmed the elemental AgNPs presence and also in agreement with the XRD analysis. The standard crystallite size of the CvAgNPs was estimated at 40.06 nm (Fig. 6A–C). The TEM picture demonstrated the cross-section borders between the two adjoining planes to be 5 nm separated which compares to the interplanar detachment of the [111] plane of face-focused cubic silver (Bhakya et al. 2016).

FT-IR spectra in Fig. 7A–C indicated the presence of phytochemicals which may be responsible for the synthesis of AgNPs from an aqueous extract from *C. viscosa*. Fig. 7A indicates the FT-IR spectra of 1mMCvAgNPs, the highest peak at 3738.82, 3458.88 and 2361.83 cm^{-1} attributed to O—H stretch, N—H stretch and O═C═O stretching vibration of alcohol, phenols, primary amine and carbon-dioxide with the medium, sharp and strong intensity. The medium and low bands at 650.62, 454.52 and 425.32 cm^{-1} corresponded to C—Br stretch and C—I stretch possible of halo-compound and alkyl halides.

In Fig. 7B represents the FT-IR spectra of 2mMCvAgNPs; in this spectrum total, 8 peaks were observed. Among these peaks 3683.67 and 2175.17 cm^{-1} attributed to O—H stretch and —C≡C— stretch vibration of alcohol, phenols and alkynes compounds. The medium bands at 1503.37 and 1233.47 cm^{-1} corresponded to C—C (in–ring) stretch and C—N stretch possible of aromatics and aliphatic amines compounds. Another peak at 1089.62 cm^{-1} was assigned to the presence of amines (C—N) compounds.

In Fig. 7C represents the FT-IR spectra of 3mMCvAgNPs, the highest peaks 3678.33 and 1830.71 cm^{-1} attributed to O—H stretching (Strong, Sharp) and C═O stretching (Strong) vibration of alcohol, phenols and anhydride compounds. The other peaks at 1502.77, 1229.82 and 1089.43 cm^{-1} were assigned to the presence of aromatics (C—C (in–ring) stretching), aliphatic amines (C—N stretch) and alkyl halides (C—N, C—Cl stretch), respectively (Sasikala et al., 2015). This spectroscopic examination affirmed the nearness of phenol, alcohols, amides, aldehydes, aliphatic amines and alkyl halides have a solid bonding with Ag and furthermore assumes a noteworthy job in diminishing and capping of Ag particles for the change of Ag + into AgNPs (Jamdagni et al., 2018; Bharathi et al., 2018).

3.4. Screening of qualitative phytochemicals

The results of qualitative phytochemical screening of synthesized CvAgNPs are shown in (Table 2). Phytochemical profile of synthesized 1mMCvAgNPs, 2mMCvAgNPs and 3mMCvAgNPs revealed the presence of saponins, steroids, phenol, coumarins

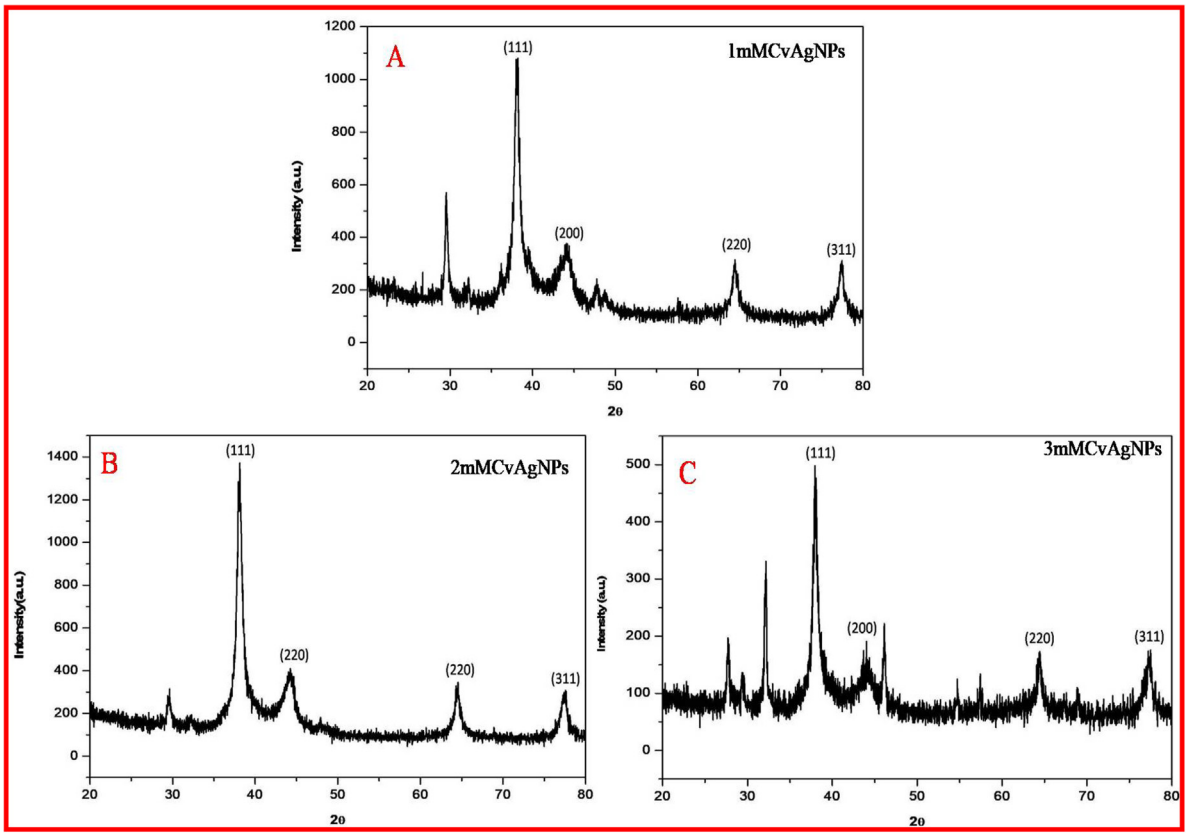

Fig. 3. XRD spectra of (**A**) 1mMCvAgNPs, (**B**) 2mMCvAgNPs and (**C**) 3mMCvAgNPs.

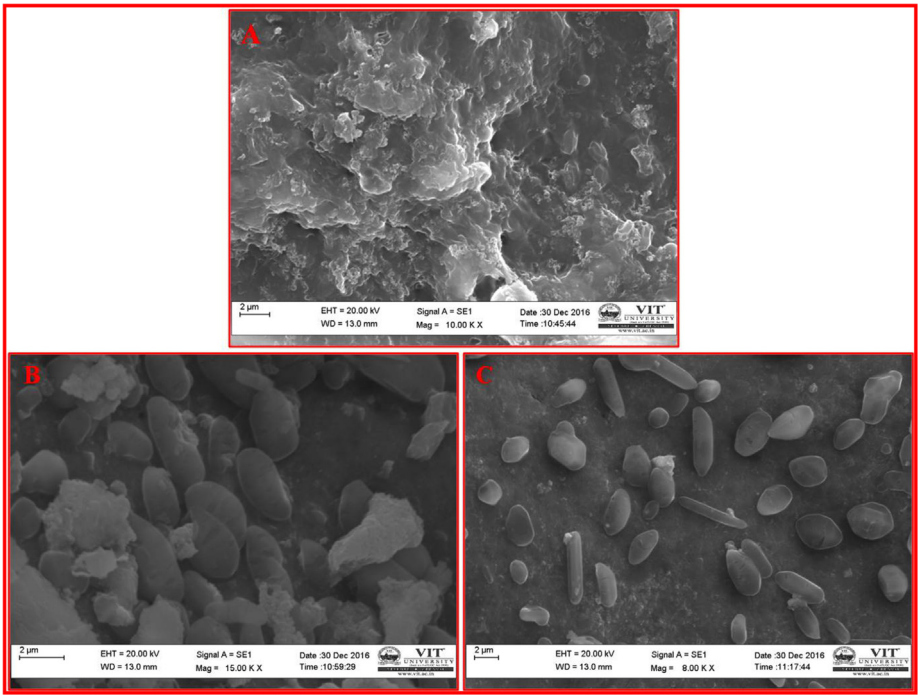

Fig. 4. SEM images of synthesized (A) 1mMCvAgNPs (B) 2mMCvAgNPs and (C) 3mMCvAgNPs.

and flavonoids which may be responsible for the efficient capping and stabilization of nanoparticles and this was further confirmed by FT-IR spectrum. Our outcomes are confirmed with the results of Devi et al. (2019).

3.5. Determination of TPC and TFC in synthesized CvAgNPs

In the obtained TPC (23.62 ± 1.21, 38.44 ± 2.76 and 67.73 ± 3.77 GAE mg/g of CvAgNPs) and TFC (46.85 ± 1.84, 56.49 ± 1.88 and

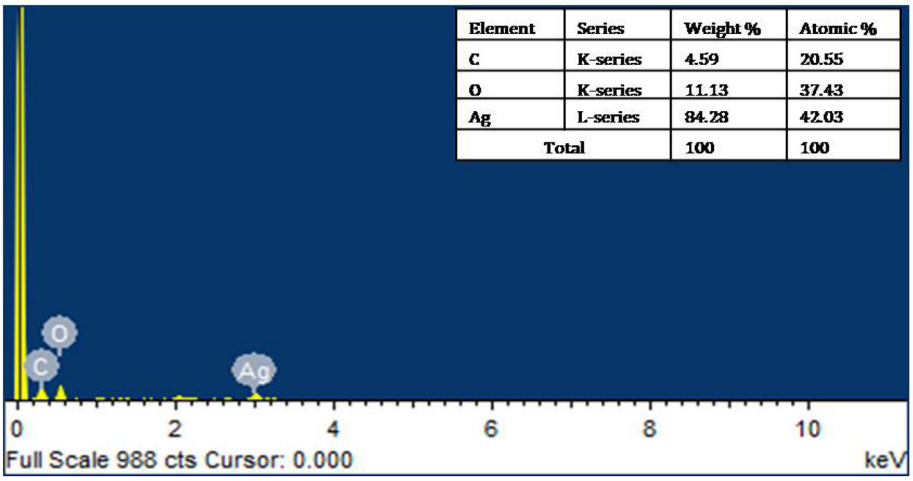

Fig. 5. EDX pattern of synthesized CvAgNPs.

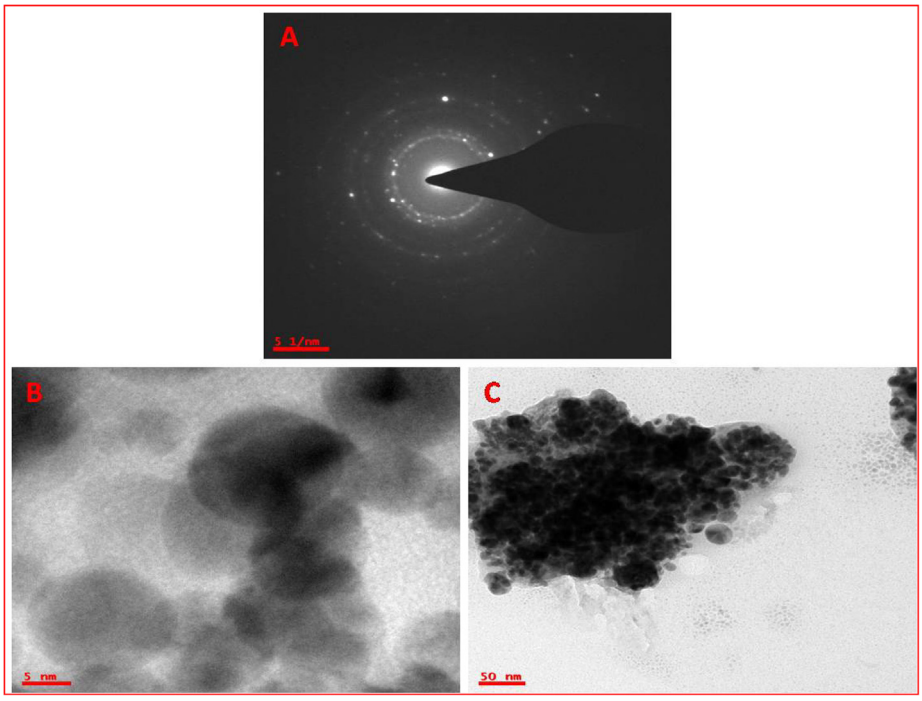

Fig. 6. TEM micrograph. Size of (A) 1mMCvAgNPs, (B) 2mMCvAgNPs and (C) 3mMCvAgNPs with SAED pattern.

85.95 ± 3.13 QRE mg/g of CvAgNPs) in the synthesized 1mMCvAgNPs, 2mMCvAgNPs and 3mMCvAgNPs were represented in Fig. 8. Dissimilar type of phytochemical constituents with a numerous functional group, which perform as reducing agents for Ag^+ ions to AgNPs. Synthesized AgNPs from the leaf (Singh et al., 2019) and seeds (Deshmukh et al., 2019) have the potential for reduction of Ag^+ ions to AgNPs.

3.6. Antibacterial activity of synthesized CvAgNPs

Antibacterial activity was performed by using 1mMCvAgNPs, 2mMCvAgNPs and 3mMCvAgNPs showed significant zone of inhibition against all the clinical isolated bacterial pathogens (Figs. 9 and 10). The 3mMCvAgNPs showed maximum zone of inhibition against *K. pneumoniae*, *P. aeruginosa*, *E. coli* and *P. putida* (Gram negative) and *S. aureus* (Gram positive) at 10 mg/mL while 1mMCvAgNPs exhibited minimum zone of inhibition. In our study, the synthesized CvAgNPs demonstrated maximum zone of inhibition against Gram negative bacterial pathogens (*K. pneumoniae*, *P. aeruginosa* and *P. putida*) compared to Gram positive bacterial pathogen (*S. aureus*). The distinction in affectability of Gram positive and Gram-negative micro-organisms to CvAgNPs was due to the distinction in thickness and constituents of their film structure (Dakal et al., 2016). Our present results are in accordance with the previous findings which demonstrate the biosynthesized AgNps have shown strong antibacterial activity. (Pirtarighat et al., 2019).

3.7. In vitro antioxidant activity of synthesized CvAgNPs

Antioxidants attract a particular interest as they can protect the human body from free radicals and prevent commencement of the degenerative diseases. Furthermore, they have the potential for

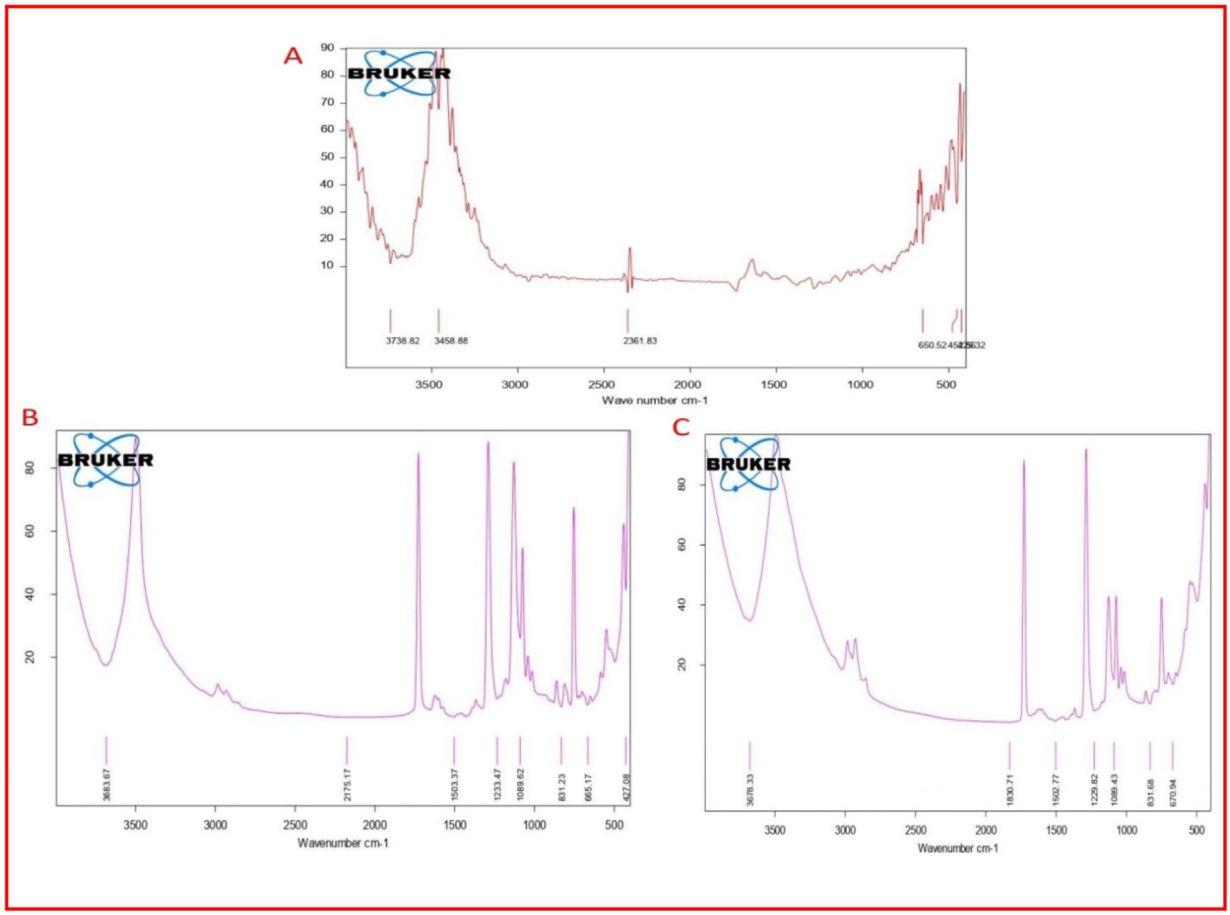

Fig. 7. FT-IR spectra of the synthesized (A) 1mMCvAgNPs (B) 2mMCvAgNPs and (C) 3mMCvAgNPs.

Table 2
Screening of phytochemicals of biosynthesized CvAgNPs.

Phytochemicals	1mMCvAgNPs	2mMCvAgNPs	3mMCvAgNPs
Alkaloids	–	–	–
Anthraquinones	–	–	–
Carbohydrates	–	–	–
Coumarins	+	+	+
Flavonoids	+	+	+
Gums	–	–	–
Glycosides	–	–	–
Oils and fates	–	–	–
Proteins and amino acids	–	–	–
Saponins	+	+	+
Steroids	+	+	+
Phenols	+	+	+
Reducing sugars	–	–	–
Tannins	–	–	–

+ Sign means presence and −Sign signifies non-appearance.

considerable investment resources at the expense of health care. Different methods were used to investigate the antioxidant property of samples like plant extracts, synthetic antioxidants, diets, vegetables etc. (Alam et al., 2013). Previous reports stated that the green synthesis, characterization and assessment of antioxidant action of silver nanoparticles from *Cestrum nocturnum* and spice blend extracts (Keshari et al., 2018; Otunola and Afolayan, 2018). The present examination was to investigate the antioxidant property of synthesized CvAgNPs.

DPPH is a stable free radical well-known for its role in reducing the acceptance of hydrogen or electron from donors. The DPPH scavenging activity of the CvAgNPs was studied based on colour change. CvAgNPs exhibited good DPPH scavenging property when compared to gallic acid (Fig. 11). Hence, the 3mMCvAgNPs had revealed higher inhibition by 92.88% DPPH scavenging activity while 1mMCvAgNPs had shown less inhibition (88.27%) and 2mMCvAgNPs had shown moderate inhibition (89.58%) of DPPH radical scavenging activity (Fig. 11). Percentage of DPPH scavenging activity of these CvAgNPs was in dose-dependent. Similar type of results were also noticed in the IC_{50} values (1mMCvAgNPs: 35.58 ± 4.37 μg/mL; 2mMCvAgNPs: 26.46 ± 1.94 μg/mL and 2mMCvAgNPs: 20.32 ± 1.33 μg/mL) (Fig. 12). The changing of colour was might be to scavenging the DPPH due to contribution of hydrogen or stable electron in the DPPH particle is responsible later than the addition of CvAgNPs into the solution of DPPH (Kanipandian et al., 2014). The DPPH scavenging potential of CvAgNPs might be attributed to the functional groups stick on to them which were initiated as of the whole plant aqueous extract.

The biosynthesized CvAgNPs were additionally scrutinized for their antioxidative prospective according to the assay of ABTS free radical scavenging study; the results are displayed in Fig. 11 and Fig. 12. The maximum ABTS radical scavenging activity of CvAgNPs at the three different concentrations (1 mM, 2 mM and 3 mM) showed of 67.83%, 71.89% and 77.63%, whereas ascorbic acid showed 83.66% at 100 μg/mL. The IC_{50} values of three concentrations of CvAgNPs were 67.4 ± 2.41 (1 mM), 64.66 ± 2.09 (2 mM) and 48.5 ± 1.25 μg/mL (3 mM) respectively. The outcomes exhibit the assurance of huge bioactive molecules of *C. viscosa* whole plant aqueous extract on the layer of the synthesized AgNPs, which are increased in the ABTS radicals scavenging efficiencies.

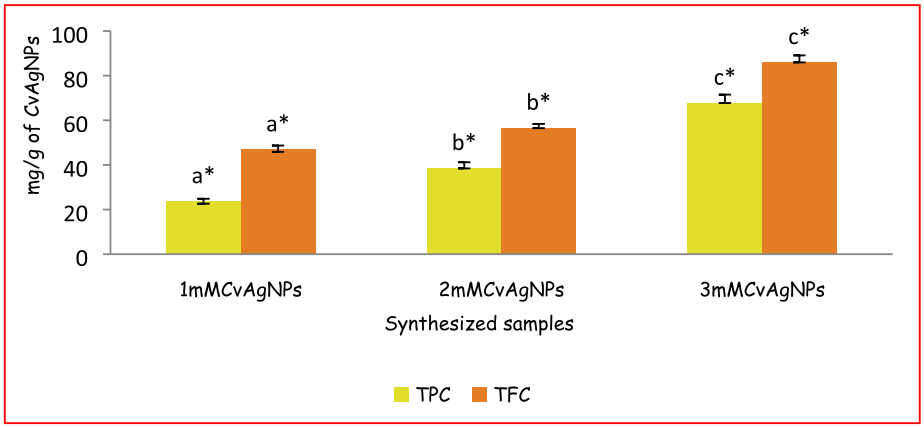

Fig. 8. TPC and TFC in the synthesized CvAgNPs. Each vertical bar represents the mean ± SE (n = 3). The vertical bars with similar colour and having the same alphabet do not differ significantly whereas the bars with similar colour and having the different alphabet differ significantly at $p < 0.05$. (One Way ANOVA followed by Tukey's post hoc test).

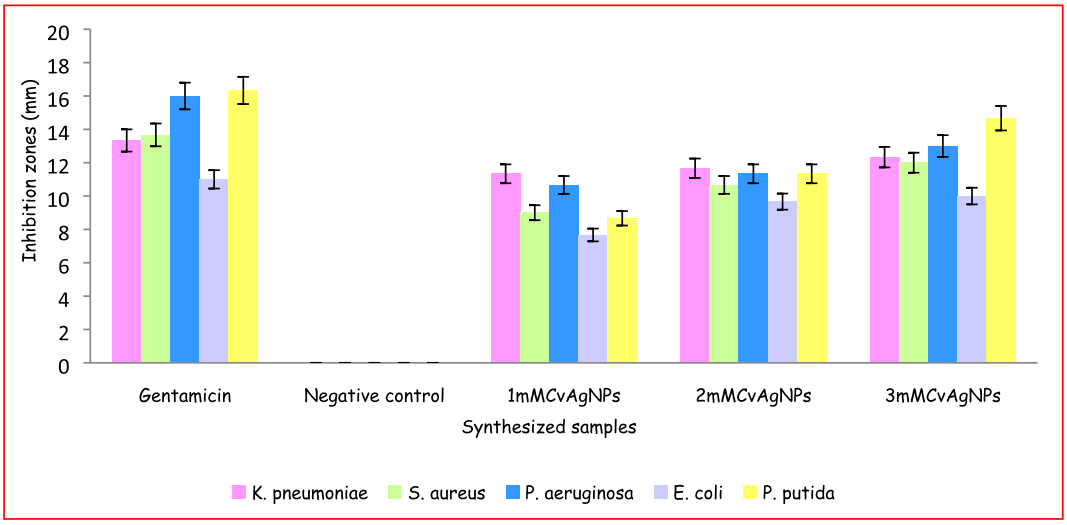

Fig. 9. Zone of inhibition of synthesised CvAgNPs against *K. pneumoniae*, *S. aureus*, *P. aeruginosa*, *E. coli* and *P. putida*. Data are representing mean ± SE (n = 3).

Khoshnamvand et al., (2019) in their investigation established that the analysis of the correlation between polyphenolic compounds of *Allium ampeloprasum* and the antioxidant movement showed that polyphenolic compounds contribute significantly to the antioxidant movement.

H_2O_2 is estimated as one of the significant agentsof cell growth and could attack various cell vitality generating frameworks (Liu et al., 2013). H_2O_2 is formed due to the result of respiration in every living cell and must be removed from the cell as it is harmful. Cells produce enzyme catalases to remove from H_2O_2. H_2O_2 scavenging action dependent on the polyphenolic substance present in the synthesized CvAgNPs, which can give electrons to H_2O_2 thus neutralize it to water. The maximum percentage of H_2O_2 scavenging activity was noticed in 3mMCvAgNPs (76.17%) while 1mMCvAgNPs (64.48%) was inhibited the low level of H_2O_2 when compared to standard gallic acid (78.26%). The IC_{50} values of three concentrations of CvAgNPs were 76.61 ± 2.57 (1 mM), 70.13 ± 1.6 (2 mM) and 62.45 ± 1.9 μg/mL (3 mM) also exhibited same movement (Fig. 12). This activity was shown in a dose-dependent manner.

Total antioxidant capacity (TAC) of the three different concentrations of synthesized CvAgNPs was also evaluated by the standard phosphomolybdenum method (Figs. 11 and 12). This method is based on the reduction of isopolymolybdate complexes, polyoxometalates containing blue colored Mo (VI) to Mo (V) by the CvAgNPs ensuing in the development of a green colored complex (phosphomolybdenum). Higher TAC power was shown by 3mMACvAgNPs (67.68 ± 2.73 μg/mL) than the remaining 1mMCvAgNPs (116.14 ± 5.46 μg/mL) and 2mMCvAgNPs (96.72 ± 3.73 μg/mL) while standard ascorbic acid was shown 48. 37 ± 2.66 μg/mL. Our results were resembled previous reports on leaf extract-mediated biocompatible AgNPs from *Pteris tripartita* (Baskaran et al., 2016).

Fig. 13 showed the dose-dependent response for the reducing powers of the biosynthesized CvAgNPs. Reducing power increased consistently with increasing the concentration of CvAgNPs-20–10 0 μg/mL. Among three concentrations of CvAgNPs, 3mMCvAgNPs exhibited high reducing power near to standard (gallic acid) due to the presence of polyphenols and functional groups in the CvAgNPs. Remaining two concentrations of synthesized AgNPs have shown the moderate and low reducing power activity. However, these polyphenols have shown electron-donating capacity (Chen et al., 2020). This result was correlated with biosynthesized AgNPs of *Prosopis farcta* fruit extract (Salari et al., 2019).

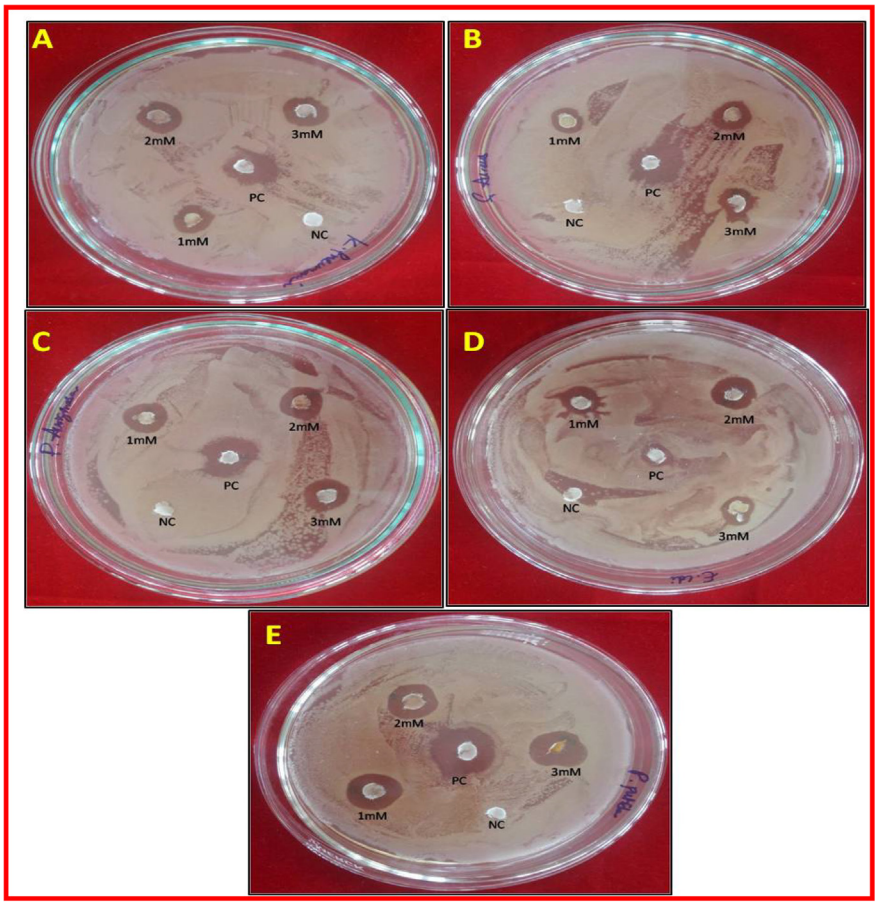

Fig. 10. Bactericidal activity of synthesized 1mMCvAgNPs, 2mMCvAgNPs, 3mMCvAgNPs and gentamycin against (A). *K. pneumoniae*, (B). *S. aureus*, (C). *P. aeruginosa*, (D). *E. coli* and (E). *P. putida*. NC– Negative control (Distilled Water); PC-Positive control (Gentamycin).

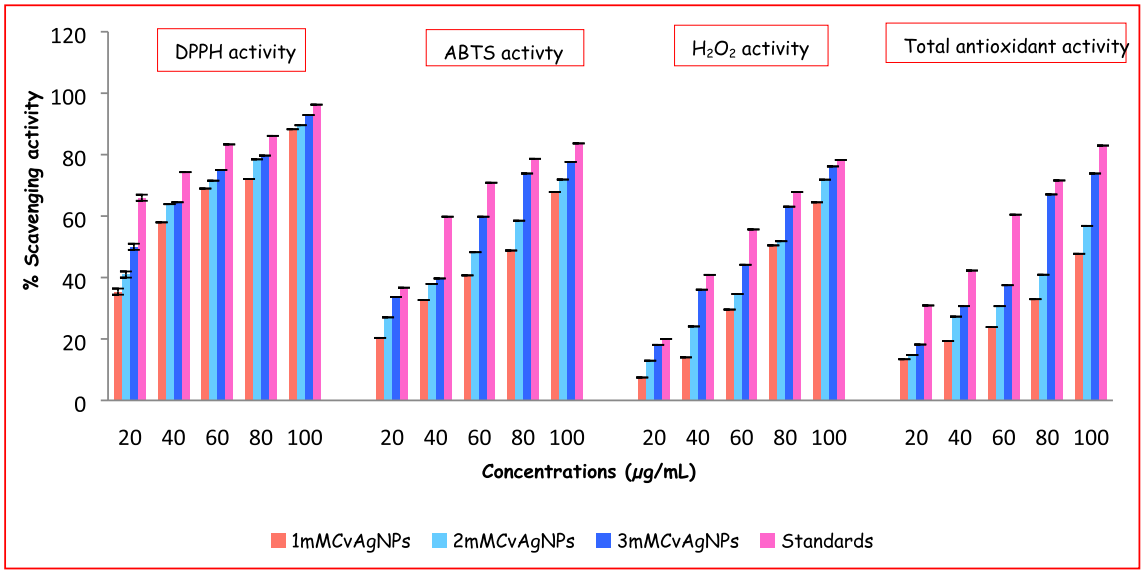

Fig. 11. Percentage of DPPH, ABTS, H_2O_2 radical scavenging activity and total antioxidant capacity (TAC) of the biosynthesized CvAgNPs.

3.8. In vitro antidiabetic activity of synthesized CvAgNPs

In the stomach, starch related enzymes i.e. pancreatic α-amylase and intestinal α-glucosidase, are responsible for the breakdown of polysaccharides and disaccharides into monosaccharides appropriate for absorption (Sales et al., 2012). Control of these two enzymes is valuable for the treatment of type-2/NIDDM, since they will control the levels of blood glucose (Podsedek et al., 2014). The CvAgNPs have potentially inhibited the activities of α-amylase and α-glucosidase enzymes in a dose-dependent

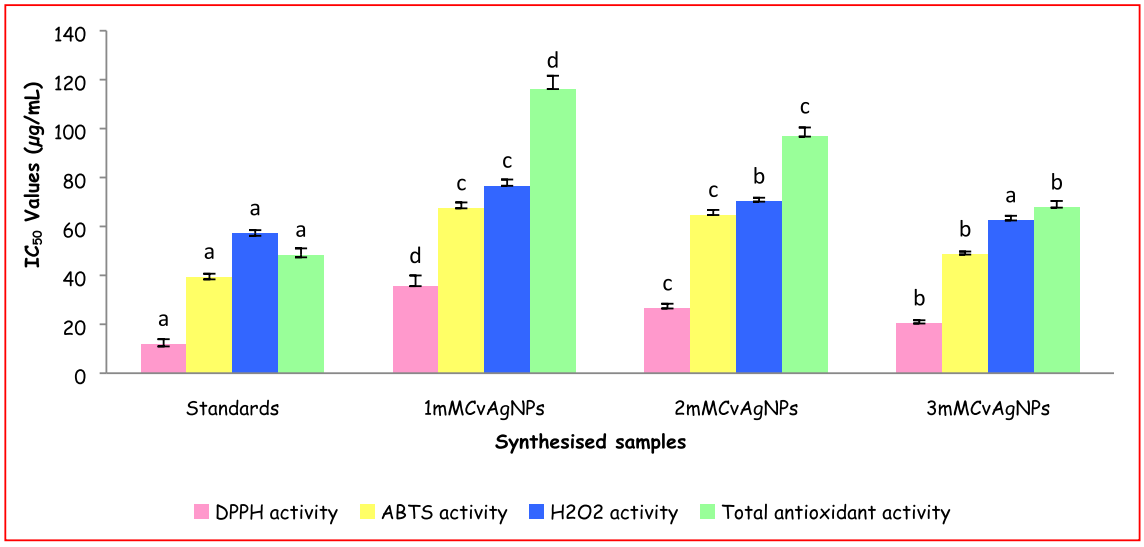

Fig. 12. IC_{50} values of DPPH, ABTS, H_2O_2 scavenging activity and total antioxidant activity of synthesized CvAgNPs. Each vertical bar represents the mean ± SE (n = 3). The vertical bars with similar colour and having the same alphabet do not differ significantly whereas the bars with similar colour and having the different alphabet differ significantly at $p < 0.05$. (One Way ANOVA followed by Tukey's post hoc test).

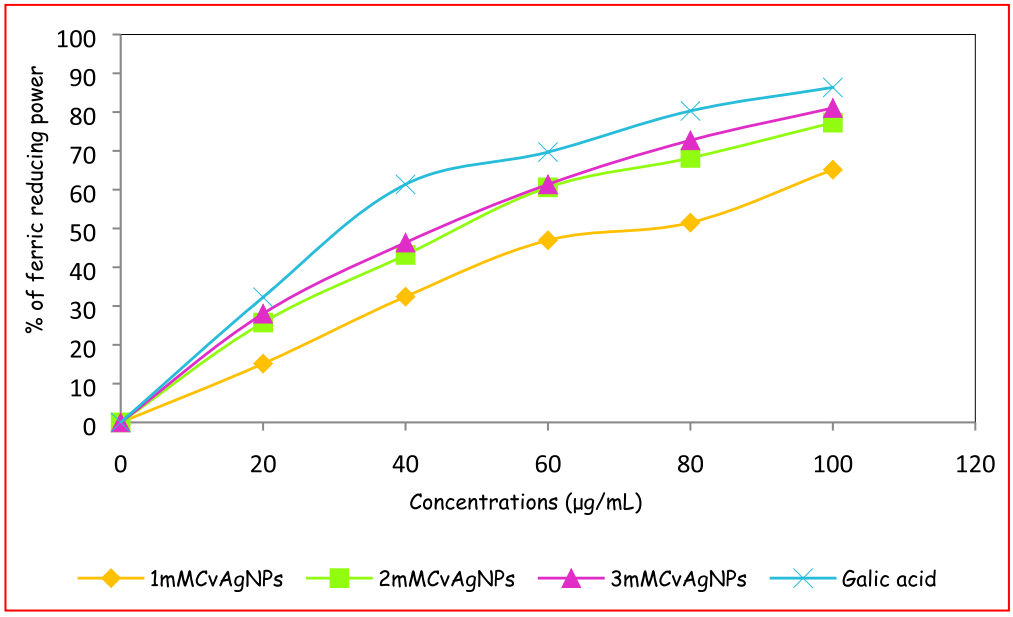

Fig. 13. Ferric reducing antioxidant power capacity of biosynthesized CvAgNPs.

manner (20–100 µg/mL) (Fig. 14). Compared with the standard acarbose, the 3mMCvAgNPs showed significantly high inhibition activity (57.62%; 90.14%), while the 2mMCvAgNPs showed moderate inhibition activity (56.98%; 81.62%) and 1mMCvAgNPs showed low inhibition activity (46.92%; 78.14%) in both α-amylase and α-glucosidase enzymes. The IC_{50} values of acarbose (14.06 ± 0.89; 18.52 ± 1.23 µg/mL), 1mMCvAgNPs (53.72 ± 2.11; 55.91 ± 2.98 µg/mL), 2mMCvAgNPs (42.44 ± 2.68; 37.73 ± 2.05 µg/mL) and 3mMCvAgNPs (21.92 ± 1.74; 21.76 ± 1.91 µg/mL) of α-amylase and α-glucosidase inhibition activity were graphically represented in Fig. 15. CvAgNPs have shown high inhibition on α-glucosidase activity when compared to α-amylase activity. The AgNPs diminished the levels of enzymes, which are in charge of catalyzing the hydrolysis of complex carbohydrates and increased the utilization rate of glucose reported by Balan et al., (2016), and Sengottaiyan et al. (2016).

The results obtained for the HbA1c assay are presented in the graphical representation in Figs. 14 and 15. The percentage inhibition of HbA1c is dose-dependent as shown in Fig. 14. The percentage of inhibition at the concentrations of 20, 40, 60, 80 and 100 µg/mL by the CvAgNPs showed a dose-dependent reduction. The highest concentration 100 µg/mL of 1mMCvAgNPs, 2mMCvAgNPs, 3mMCvAgNPs and metformin showed a maximum inhibition of 26.12, 27.96, 32.68 and 36.89% respectively while the lowest concentration 20 µg/mL of 1mMCvAgNPs, 2mMCvAgNPs, 3mMCvAgNPs and metformin showed a minimum inhibition of 2.78, 3.68, 10.81 and 15.40% respectively. The IC_{50} values of the synthesized CvAgNPs and standard were found to be 175.17 ± 14.13, 177.69 ± 15.65, 164.19 ± 10.91 and 159.31 ± 9.9 µg/mL respectively. Similar results were found in biologically synthesized AgNPs from *Pouteria sapota* (Prabhu et al., 2018).

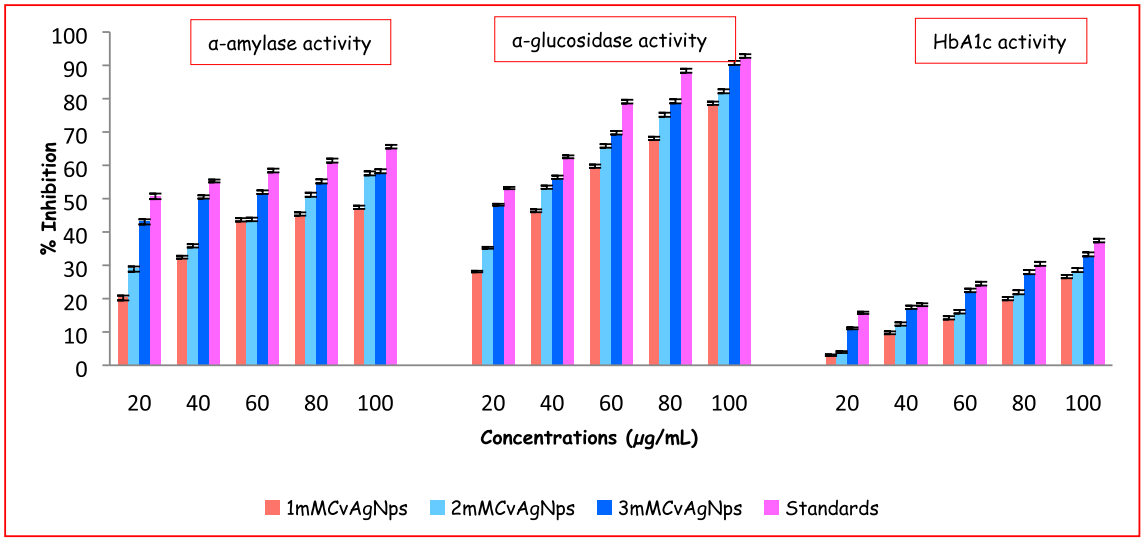

Fig. 14. Inhibition activity of CvAgNPs on α-amylase, α-glucosidase and HbA1c.

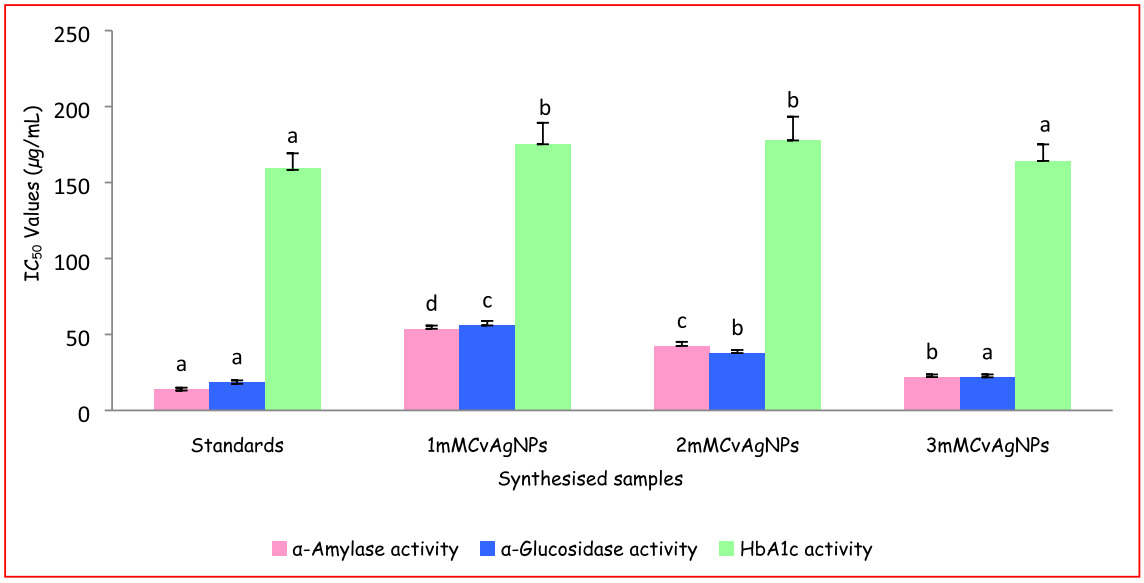

Fig. 15. IC_{50} values of α- amylase, α-glucosidase and HbA1c inhibitory activity of synthesized CvAgNPs. Each vertical bar represents the mean ± SE (n = 3). The vertical bars with similar colour and having the same alphabet do not differ significantly whereas the bars with similar colour and having the different alphabet differ significantly at $p < 0.05$. (One Way ANOVA followed by Tukey's post hoc test).

This study indicates that the synthesized CvAgNPs showed high inhibition activity against α-glucosidase and α-amylase than acarbose. In addition, CvAgNPs showed significant antibacterial and antioxidant activities due to the rich amount of phenolic and flavonoid content present in synthesized CvAgNPs. A few studies have reported biological activities such as antimicrobial, antioxidant and antidiabetic activity of *Pisum sativum* (Patra et al., 2019), *Ipomoea batatas* (Das et al., 2019), *Lysimachia foenumgraecum* (Chartarrayawadee et al., 2020) and *Ribes nigrum* (Vorobyova et al., 2020).

4. Conclusions and recommendations

Synthesis of AgNPs from the biological agent is eco-friendly, low-cost and proficient to synthesis at room temperature. The current research is developed an easy and eco-friendly method for the synthesis of three different concentrations of silver nanoparticles (1mMCvAgNPs, 2mMCvAgNPs and 3mMCvAgNPs) using aqueous whole plant extract of *Cleome viscosa*. We have characterized the synthesized CvAgNPs using UV–vis spectroscopy, XRD, SEM, TEM and FTIR analysis. The spectra of UV–vis confirmed the biosynthesized CvAgNPs supporting on surface plasmon resonance reading. XRD spectra confirmed the structure of FCC and crystalline nature in AgNPs. The reducing and capping of AgNPs are due to the presence of phytochemicals, which was confirmed by FT-IR spectra analysis. The SEM monograph revealed rod-shaped, spherical, and triangular-shaped AgNPs. TEM micrograph displayed different shapes of synthesized AgNPs like rod-shaped, spherical, and triangular in shape with size between 5 and 50 nm. The synthesized CvAgNPs demonstrated maximum antibacterial activity against

Gram negative bacterial pathogens (*K. pneumoniae*, *P. aeruginosa* and *P. putida*) compared to Gram positive bacteria pathogen (*S. aureus*). The synthesized CvAgNPs demonstrated favorable antioxidant activity against DPPH, ABTS, H_2O_2 free radicals and also shown high TAC and RP. The CvAgNPs also showed good antidiabetic activity against α-amylase, α-glucosidase and HbA1c. The outcome of the present study confirms that the phytochemicals and polyphenols are in charge of the whole plant *of C. viscosa* aqueous extract for the synthesis of AgNPs and demonstrated effective biological actions attempted. Thus, this safe and eco-friendly synthesis process can be used for the development of AgNPs which also demonstrate effective biological properties in the future. Further studies are necessary in order to get more applications of these biosynthesized AgNPs.

Declaration of Competing Interest

The authors declare that they have no known competing financial interests or personal relationships that could have appeared to influence the work reported in this paper.

Acknowledgements

We thank all the authors for their support and help and also, we thank the Centre for Organic and Medicinal Chemistry, VIT University, Vellore, India for providing research facilities and Prof. N. Yasodamma (S.V. University, Tirupati, India) for plant Authentication.

References

Ahmed, R.H., Mustafa, D.E., 2020. Green synthesis of silver nanoparticles mediated by traditionally used medicinal plants in Sudan. Int. Nano Lett. 10, 1–14.
Alam, M.N., Bristi, N.J., Rafiquzzaman, M., 2013. Review on in vivo and in vitro methods evaluation of antioxidant activity. Saudi Pharm. J. 21, 143–152.
Al-Owaisi, M., Al-Hadiwi, N., Khan, S.A., 2014. GC-MS analysis, determination of total phenolics, flavonoid content and free radical scavenging activities of various crude extracts of *Moringa peregrina* (Forssk.) Fiori leaves. Asian Pac. J. Trop Biomed. 4, 964–970.
Anandalakshmi, K., Venugobal, J., Ramasamy, V., 2016. Characterization of silver nanoparticles by green synthesis method using *Pedalium murex* leaf extract and their antibacterial activity. Appl. Nanosci. 6, 399–408.
Ashraf, J.M., Ansari, M.A., Khan, H.M., Alzohairy, M.A., Choi, I., 2016. Green synthesis of silver nanoparticles and characterization of their inhibitory effects on AGEs formation using biophysical techniques. Sci. Rep. 6, 204–214.
Balan, K., Qing, W., Wang, Y., Liu, X., Palvannan, T., Wang, Y., Ma, F., Zhang, Y., 2016. Antidiabetic activity of silver nanoparticles from green synthesis using *Lonicera japonica* leaf extract. Rsc Adv. 6, 40162–40168.
Balavijayalakshmi, J., Ramalakshmi, V., 2017. Carica papaya peel mediated synthesis of silver nanoparticles and its antibacterial activity against human pathogens. J. Appl. Res. Technol. 15, 413–422.
Baskaran, X., Vigila, A.V.G., Parimelazhagan, T., Muralidhara-Rao, D., Zhang, S., 2016. Biosynthesis, characterization, and evaluation of bioactivities of leaf extract-mediated biocompatible silver nanoparticles from an early tracheophyte, *Pteris tripartita* sw. Int. J. Nanomed. 11, 5789.
Behravan, M., Panahi, A.H., Naghizadeh, A., Ziaee, M., Mahdavi, R., Mirzapour, A., 2019. Facile green synthesis of silver nanoparticles using Berberis vulgaris leaf and root aqueous extract and its antibacterial activity. Int. J. Biol. Macromol. 124, 148–154.
Bhakya, S., Muthukrishnan, S., Sukumaran, M., Muthukumar, M., 2016. Biogenic synthesis of silver nanoparticles and their antioxidant and antibacterial activity. Appl. Nanosci. 6, 755–766.
Bharathi, D., Josebin, M.D., Vasantharaj, S., Bhuvaneshwari, V., 2018. Biosynthesis of silver nanoparticles using stem bark extracts of *Diospyros montana* and their antioxidant and antibacterial activities. J. Nanostruct. Chem. 8, 83–92.
Brand-Williams, W., Cuvelier, M.E., Berset, C.L.W.T., 1995. Use of a free radical method to evaluate antioxidant activity. LWT-Food Sci. Technol. 28, 25–30.
Chang, C.C., Yang, M.H., Wen, H.M., Chern, J.C., 2002. Estimation of total flavonoid content in propolis by two complementary colorimetric methods. J. Food Drug Anal. 10 (3).
Chartarrayawadee, W., Charoensin, P., Saenma, J., Rin, T., Khamai, P., Nasomjai, P., Too, C.O., 2020. Green synthesis and stabilization of silver nanoparticles using Lysimachia foenum-graecum Hance extract and their antibacterial activity. Green Process Synth. 9, 107–118.
Chaudhari, K., Ahuja, T., Murugesan, V., Subramanian, V., Ganayee, M.A., Thundat, T., Pradeep, T., 2019. Appearance of SERS activity in single silver nanoparticles by laser-induced reshaping. Nanoscale. 11, 321–330.
Chaudhari, M.G., Joshi, B.B., Mistry, K.N., 2013. *In vitro* anti-diabetic and anti-inflammatory activity of stem bark of *Bauhinia purpurea*. Bull. Pharmaceut. Med. Sci. (BOPAMS) 1 (2).
Chen, J., Yang, J., Ma, L., Li, J., Shahzad, N., Kim, C.K., 2020. Structure-antioxidant activity relationship of methoxy, phenolic hydroxyl, and carboxylic acid groups of phenolic acids. Sci. Rep. 10, 1–9.
Dakal, T.C., Kumar, A., Majumdar, R.S., Yadav, V., 2016. Mechanistic basis of antimicrobial actions of silver nanoparticles. Front Microbiol. 7, 1831.
Das, G., Patra, J.K., Nagaraj Basavegowda, C.N.V., Shin, H.S., 2019. Comparative study on antidiabetic, cytotoxicity, antioxidant and antibacterial properties of biosynthesized silver nanoparticles using outer peels of two varieties of Ipomoea batatas (L.) Lam. Int. J. Nanomed. 14, 4741.
Deshmukh, A.R., Gupta, A., Kim, B.S., 2019. Ultrasound Assisted Green Synthesis of Silver and Iron Oxide Nanoparticles Using Fenugreek Seed Extract and Their Enhanced Antibacterial and Antioxidant Activities. Biomed Res. 2019.
Devi, M., Devi, S., Sharma, V., Rana, N., Bhatia, R.K., Bhatt, A.K., 2019. Green synthesis of silver nanoparticles using methanolic fruit extract of *Aegle marmelos* and their antimicrobial potential against human bacterial pathogens. J. Tradit Complement. Med. 1.
Evans, W. C., 2002. Trease and Evans Pharmacognosy. 15thedn. Sanders Co. Ltd. Singapore, 2002.
Facciola. S., Kampong Publications, 1990. Cornucopia - A Source Book of Edible Plants.
Govindappa, M., Hemashekhar, B., Arthikala, M.K., Rai, V.R., Ramachandra, Y.L., 2018. Characterization, antibacterial, antioxidant, antidiabetic, anti-inflammatory and antityrosinase activity of green synthesized silver nanoparticles using *Calophyllum tomentosum* leaves extract. Results Phys. 9, 400–408.
Hansawasdi, C., Kawabata, J., Kasai, T., 2000. α-Amylase inhibitors from roselle *(Hibiscus sabdariffa* Linn.) tea. Biosci. Biotechnol. Biochem. 64, 1041–1043.
Hembram, K.C., Kumar, R., Kandha, L., Parhi, P.K., Kundu, C.N., Bindhani, B.K., 2018. Therapeutic prospective of plant-induced silver nanoparticles: application as antimicrobial and anticancer agent. Artif. Cells Nanomed. Biotechnol. 46, S38–S51.
Iravani, S., Korbekandi, H., Mirmohammadi, S.V., Zolfaghari, B., 2014. Synthesis of silver nanoparticles: chemical, physical and biological methods. Res. Pharm. Sci. 9, 385.
Ismail, R.A., Sulaiman, G.M., Mohsin, M.H., Saadoon, A.H., 2018. Preparation of silver iodide nanoparticles using laser ablation in liquid for antibacterial applications. IET Nanobiotechnol. 12, 781–786.
Jamdagni, P., Khatri, P., Rana, J.S., 2018. Green synthesis of zinc oxide nanoparticles using flower extract of Nyctanthes arbor-tristis and their antifungal activity. J. King Saud Univ. Sci. 30, 168–175.
Jyoti, K., Baunthiyal, M., Singh, A., 2016. Characterization of silver nanoparticles synthesized using *Urtica dioica* Linn. leaves and their synergistic effects with antibiotics. J. Radiat. Res. Appl. Sci. 9, 217–227.
Kanipandian, N., Kannan, S., Ramesh, R., Subramanian, P., Thirumurugan, R., 2014. Characterization, antioxidant and cytotoxicity evaluation of green synthesized silver nanoparticles using *Cleistanthus collinus* extract as surface modifier. Mater. Res. Bull. 49, 494–502.
Karthik, L., Gaurav, K., Rao, K.B., 2013. Environmental and human impact on marine microorganisms synthesized nanoparticles. Marine biomaterials: characterization, isolation and applications. CRC Press, Boca Raton. pp. 253–272.
Keshari, A.K., Srivastava, R., Singh, P., Yadav, V.B., Nath, G., 2018. Antioxidant and antibacterial activity of silver nanoparticles synthesized by Cestrum nocturnum. J. Ayurveda Integr. Med., 1–8
Khan, I., Saeed, K., Khan, I., 2017. Nanoparticles: Properties, applications and toxicities. Arab. J. Chem.18.
Khoshnamvand, M., Huo, C., Liu, J., 2019. Silver nanoparticles synthesized using *Allium ampeloprasum* L. leaf extract: characterization and performance in catalytic reduction of 4-nitrophenol and antioxidant activity. J. Mol. Struct. 1175, 90–96.
Kuppusamy, P., Yusoff, M.M., Maniam, G.P., Govindan, N., 2016. Biosynthesis of metallic nanoparticles using plant derivatives and their new avenues in pharmacological applications–An updated report. Saudi Pharm. J. 24, 473–484.
Lakshmanan, G., Sathiyaseelan, A., Kalaichelvan, P.T., Murugesan, K., 2018. Plant-mediated synthesis of silver nanoparticles using fruit extract of Cleome viscosa L.: Assessment of their antibacterial and anticancer activity. Karbala Int. J. Modern Sci. 4, 61–68.
Liu, J., Jia, L., Kan, J., Jin, C.H., 2013. *In vitro* and *in vivo* antioxidant activity of ethanolic extract of white button mushroom (*Agaricus bisporus*). Food Chem. Toxicol. 51, 310–316.
Manandhar, N.P., 2002. Plants and people of Nepal. Timber press.
Nagababu, P., Rao, V.U., 2017. Pharmacological assessment, green synthesis and characterization of silver nanoparticles of *Sonneratia apetala* buch.-ham. leaves. J. Appl. Pharm. Sci. 7, 175–182.
Nguyen, T.P., Tran, C.L., Vuong, C.H., Do, T.H.T., Le, T.D., Mai, D.T., Phan, N.M., 2017. Flavonoids with hepatoprotective activity from the leaves of *Cleome viscosa* L. Nat. Prod. Res. 31, 2587–2592.
Oluwaniyi, O.O., Adegoke, H.I., Adesuji, E.T., Alabi, A.B., Bodede, S.O., Labulo, A.H., Oseghale, C.O., 2016. Biosynthesis of silver nanoparticles using aqueous leaf extracts of *Thevetia peruviana* Juss and its antimicrobial activities. Appl. Nanosci. 6, 903–912.

Otunola, G.A., Afolayan, A.J., 2018. *In vitro* antibacterial, antioxidant and toxicity profile of silver nanoparticles green-synthesized and characterized from aqueous extract of a spice blend formulation. Biotechnol. Biotec. Eq. 32, 724–733.

Oyaizu, M., 1986. Studies on products of browning reaction. Japanese J. Nutrit. Dietetics 44, 307–315.

Pannerselvam, B., Durai, P., Thiyagarajan, D., Song, H.J., Kim, K.J., Jung, Y.S., Kim, H.J., Rangarajulu, S.K., 2020. Facile synthesis of silver nanoparticles using Asian spider flower and its in vitro cytotoxic activity against human breast carcinoma cells. Processes 8, 430.

Patra, J.K., Das, G., Shin, H.S., 2019. Facile green biosynthesis of silver nanoparticles using Pisum sativum L. outer peel aqueous extract and its antidiabetic, cytotoxicity, antioxidant, and antibacterial activity. Int. J. Nanomed.. 14, 6679.

Pirtarighat, S., Ghannadnia, M., Baghshahi, S., 2019. Green synthesis of silver nanoparticles using the plant extract of *Salvia spinosa* grown in vitro and their antibacterial activity assessment. J. Nanostruct. Chem. 9, 1–9.

Podsedek, A., Majewska, I., Redzynia, M., Sosnowska, D., Koziołkiewicz, M., 2014. *In vitro* inhibitory effect on digestive enzymes and antioxidant potential of commonly consumed fruits. J. Agric. Food Chem. 62, 4610–4617.

Prabhu, S., Vinodhini, S., Elanchezhiyan, C., Rajeswari, D., 2018. Evaluation of antidiabetic activity of biologically synthesized silver nanoparticles using *Pouteria sapota* in streptozotocin-induced diabetic rats. J. Diabetes. 10, 28–42.

Prieto, P., Pineda, M., Aguilar, M., 1999. Spectrophotometric quantitation of antioxidant capacity through the formation of a phosphomolybdenum complex: specific application to the determination of vitamin E. Anal. Biochem. 269, 337–341.

Quaresma, P., Soares, L., Contar, L., Miranda, A., Osório, I., Carvalho, P.A., Franco, R., Pereira, E., 2009. Green photocatalytic synthesis of stable Au and Ag nanoparticles. Green Chem. 11, 1889–1893.

Rai, M., Kon, K., Ingle, A., Duran, N., Galdiero, S., Galdiero, M., 2014. Broad-spectrum bioactivities of silver nanoparticles: the emerging trends and future prospects. Appl. Microbiol. Biotechnol. 98, 1951–1961.

Raja, S., Ramesh, V., Thivaharan, V., 2017. Green biosynthesis of silver nanoparticles using *Calliandra haematocephala* leaf extract, their antibacterial activity and hydrogen peroxide sensing capability. Arab. J. Chem. 10, 253–261.

Rajakumar, G., Gomathi, T., Thiruvengadam, M., Rajeswari, V.D., Kalpana, V.N., Chung, I.M., 2017. Evaluation of anti-cholinesterase, antibacterial and cytotoxic activities of green synthesized silver nanoparticles using from *Millettia pinnata* flower extract. Microb. Pathog. 103, 123–128.

Re, R., Pellegrini, N., Proteggente, A., Pannala, A., Yang, M., Rice-Evans, C., 1999. Antioxidant activity applying an improved ABTS radical cation decolorization assay. Free Radic. Biol. Med. 26, 1231–1237.

Ruch, R.J., Cheng, S.J., Klaunig, J.E., 1989. Prevention of cytotoxicity and inhibition of intercellular communication by antioxidant catechins isolated from Chinese green tea. Carcinogenesis. 10, 1003–1008.

Salari, S., Bahabadi, S.E., Samzadeh-Kermani, A., Yosefzaei, F., 2019. *In-vitro* Evaluation of Antioxidant and Antibacterial Potential of Green Synthesized Silver Nanoparticles Using *Prosopis farcta* Fruit Extract. Iran J Pharm Res. 18, 430.

Sales, P.M., Souza, P.M., Simeoni, L.A., Magalhães, P.O., Silveira, D., 2012. α-Amylase inhibitors: a review of raw material and isolated compounds from plant source. J. Pharm. Pharm. Sci. 15, 141–183.

Sasikala, A., Rao, M.L., Savithramma, N., Prasad, T.N.V.K.V., 2015. Synthesis of silver nanoparticles from stem bark of *Cochlospermum religiosum* (L.) Alston: an important medicinal plant and evaluation of their antimicrobial efficacy. Appl. Nanosci. 5, 827–835.

Selvam, K., Sudhakar, C., Govarthanan, M., Thiyagarajan, P., Sengottaiyan, A., Senthilkumar, B., Selvankumar, T., 2017. Eco-friendly biosynthesis and characterization of silver nanoparticles using *Tinospora cordifolia* (Thunb.) Miers and evaluate its antibacterial, antioxidant potential. J. Radiat. Res. Appl. Sci. 10, 6–12.

Sengottaiyan, A., Aravinthan, A., Sudhakar, C., Selvam, K., Srinivasan, P., Govarthanan, M., Manoharan, K., Selvankumar, T., 2016. Synthesis and characterization of *Solanum nigrum*-mediated silver nanoparticles and its protective effect on alloxan-induced diabetic rats. J Nanostructure Chem. 6, 41–48.

Senthamilselvi, M.M., Kesavan, D., Sulochana, N., 2012. An anti-inflammatory and anti-microbial flavone glycoside from flowers of *Cleome viscosa*. Org Med Chem Lett. 2, 19.

Sheel, R., Nisha, K., Kumar, J., 2014. Preliminary phytochemical screening of methanolic extract of *Clerodendron infortunatum*. IOSR J. Appl. Chem. 7, 10–13.

Singh, C., Kumar, J., Kumar, P., Chauhan, B.S., Tiwari, K.N., Mishra, S.K., Srikrishna, S., Saini, R., Nath, G., Singh, J., 2019. Green synthesis of silver nanoparticles using aqueous leaf extract of *Premna integrifolia* (L.) rich in polyphenols and evaluation of their antioxidant, antibacterial and cytotoxic activity. Biotechno. l Biotec. Eq. 1–13.

Singh, J., Dutta, T., Kim, K.H., Rawat, M., Samddar, P., Kumar, P., 2018. 'Green'synthesis of metals and their oxide nanoparticles: applications for environmental remediation. J. Nanobiotechnology. 16, 84.

Singleton, V.L., Rossi, J.A., 1965. Colorimetry of total phenolics with phosphomolybdic-phosphotungstic acid reagents. Am. J. Enol. Viticult. 16, 144–158.

Taha, Z.K., Hawar, S.N., Sulaiman, G.M., 2019. Extracellular biosynthesis of silver nanoparticles from *Penicillium italicum* and its antioxidant, antimicrobial and cytotoxicity activities. Biotechnol Lett. 41, 899–914.

Vorobyova, V., Vasyliev, G., Skiba, M., 2020. Eco-friendly "green" synthesis of silver nanoparticles with the black currant pomace extract and its antibacterial, electrochemical, and antioxidant activity. Appl. Nanosci. 2, 2020. https://doi.org/10.1007/s13204-020-01369-z.

Yin, Y.L., Tang, Z.R., Sun, Z.H., Liu, Z.Q., Li, T.J., Huang, R.L., Ruan, Z., Deng, Z.Y., Gao, B., Chen, L.X., Wu, G.Y., 2008. Effect of galacto-mannan-oligosaccharides or chitosan supplementation on cytoimmunity and humoral immunity in early-weaned piglets. Asian-Australas J Anim Sci. 21, 723–731.